

Identification of the Parameters of Menétrey -Willam Failure Surface of Calcium Silicate Units

Jasiński Radosław¹

¹ Silesian University of Technology, Faculty of Civil Engineering, Building Structures Department, 44-100 Gliwice, ul. Akademicka 5, Poland

radoslaw.jasinski@polsl.pl

Abstract. The identification of parameters of Menétrey-Willam surface made of concrete, masonry or autoclaved aerated concrete is not complicated. It is much more difficult to identify failure parameters of masonry units with cavities. This paper describes the concept of identifying the parameters of Menétrey-Willam failure surface (M-W-3) with reference to masonry units with vertical cavities. The M-W-3 surface is defined by uniaxial compressive strength f_c , uniaxial tensile strength f_t and eccentricity of elliptical function e . A test stand was built to identify surface parameters. It was used to test behaviour of masonry units under triaxial stress and conduct tests on whole masonry units in the uniaxial state. Results from tests on tens of silicate masonry units are presented in the Haigh-Westergaard (H-W) space. Statistical analyses were used to identify the shape of surface meridian, and then to determine eccentricity of the elliptical function.

1. Introduction

This paper presents the original concept of identifying parameters of Menétrey – Willam failure surface (M-W-3) masonry units with vertical hollows. For masonry units with vertical cavities [1, 2] with typical orthotropy, the standard pressure chambers, e.g. Hoek or Karmann type used for concrete or rock testing is completely useless. They require indirect methods based on adjusting the surface (determined on the basis of homogeneous samples collected from the masonry units) to conduct tests on cut to size masonry units [3]. Identification of failure surface based on whole elements testing is the most reliable method. However, it requires tests covering the whole masonry units subjected to triaxial stress using a test stand created just for that purpose. The masonry unit by a Polish manufacturer was used in the tests. It had a length of 0.25 m, a height of 0.24 m and a thickness of 0.18 m. Vertical holes constituted 26%.

2. Failure surface of Menétrey–Willam

The surface of Menétrey–Willam [4] is a modified version of the empirical model developed by Hoek and Brown [5] (used for rock description) changed by Weihe [6] who introduced the elliptic function of eccentricity e depending on Lode angle Θ . The final form of a criterion used in that model was elaborated by Menétrey–Willam [4] who expressed a three-parameter yield surface M-W-3 as follows:

$$f^p(\xi, \rho, \Theta) = \left(\sqrt{1,5} \frac{\rho}{k(\kappa)f_c} \right)^2 + m \left(\frac{\rho}{\sqrt{6k(\kappa)f_c}} r(\Theta, e) + \frac{\xi}{\sqrt{3k(\kappa)f_c}} \right) - c(\kappa) = 0; \quad (1)$$



where:

$$m = 3 \frac{(k(\kappa)f_c)^2 - (\lambda_t f_t)^2}{k(\kappa)f_c \lambda_t f_t} \frac{e}{e+1} \text{ – a parameter equivalent to cohesion,} \tag{2}$$

$$r(\theta, e) = \frac{4(1-e^2)\cos^2\theta + (2e-1)^2}{2(1-e^2)\cos\theta + (2e-1)\sqrt{4(1-e^2)\cos^2\theta + 5e^2 - 4e}} \text{ – elliptical function – Fig. 2,} \tag{3}$$

e – eccentricity of the elliptical function assuming values from the range $e \in (0,5;1,0)$,

f_c, f_t – uniaxial compressive and tensile strength,

$\lambda_t \geq 1$ – scaling parameter for M-W-3 surface.

The boundary surface M-W-3 in deviatory cross-section is composed of three tangential curves along compressive meridians– Fig. 1 whose shape is affected by the assumed eccentricity e of elliptical function – Fig. 2. When eccentricity e is 0.5, the deviatory cross-section of failure surface is in the shape of an equilateral triangle. For $e = 1.0$, curves forming the deviator cross section take on a shape of circle. A curve, whose shape is similar to ellipse in the zone of biaxial compression values $\sigma_1 - \sigma_2, \sigma_3 = 0$, is a track of boundary surface in the plane of principal stresses. In the hydrostatic cross-section, the surface is formed by parabolic meridians intersecting at the tension point corresponding to triaxial tension. The ellipse extreme corresponds to material strength to biaxial compression f_{bc} . Concrete strength to biaxial stress was empirically determined as $f_{bc} = 1.14f_c$, and the corresponding eccentricity of elliptical function was $e=0.52$. For masonry units, the majority of tests covered solid brick [7, 8]. The obtained values of solid brick strength to biaxial compression f_{bc} were within the range $1.02-1.14f_c$, and the corresponding eccentricity values were $e = 0.501-0.511$. The summary of triaxial test results for solid brick are shown in Table 1.

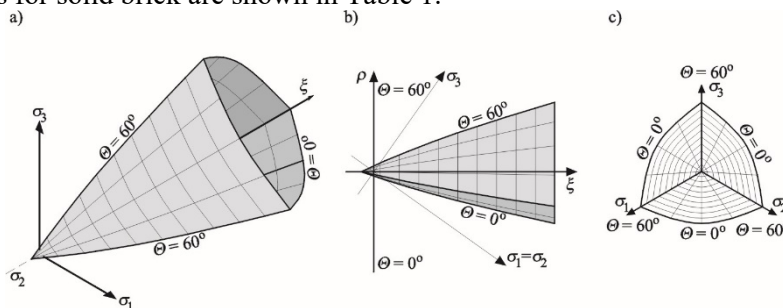


Fig. 1. Menétrey–Willam criterion in the Haigh–Westergaard space: a) the space of principal stresses, b) hydrostatic cross-section, c) deviatory cross-section

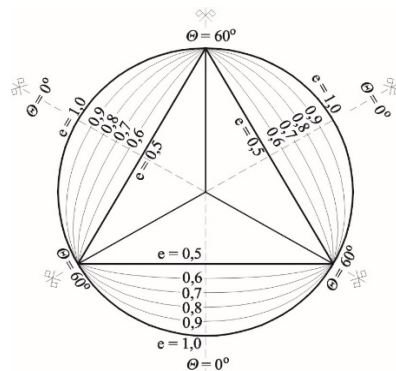


Fig. 2. Elliptical curve shape $0,5 \geq r(\theta, e) \geq 1,0$

Table 1. Results from strength tests on biaxial compression of solid brick and values of elliptic function

No.	Material	Author	Biaxial compressive strength f_{bc}	Eccentricity of elliptical function e
1	Solid brick	Drobiec [8]	$1.02 f_c$	0.501
2	Solid brick	Jasiński [7]	$1.14 f_c$	0.511

The parameter of surface adjustment $\lambda_t > 1$ determined the position of M-W-3 surfaces to the Rankine failure surface. At $\lambda_t = 1$, plasticity surface of M-W-3 was always within the Rankine pyramid, and at $\lambda_t = 2$ surfaces intersected at the plane of hydrostatic tension and minor compression.

3. Tests on masonry units exposed to triaxial stress

The whole masonry units exposed to triaxial stresses were tested using a test stand particularly built for that purpose. The test stand is shown in Fig. 3. The whole masonry unit *1* was placed on the heavy weight bases of the stand *2* located between parts of the testing machine *3*. The standard stress σ_1 perpendicular to the supporting plane of the unit was induced by a hydraulic actuator *12* with the capacity of 1000 kN, and the exerted force was measured with electro-resistant dynamometer *13* having the capacity of 2000 kN. Teflon slabs *11* were used to reduce friction on the top and bottom support area of the unit. A set of two retaining slabs *4* joined with steel rod tendons *5* having a diameter of 25 mm, was used to induce standard stresses σ_2 perpendicular to bed plane of the masonry unit. Steel brackets *6* were fixed to the plates *4*. A hydraulic actuator *8* with the capacity of 1000 kN or an electro-resistant dynamometer *9* with the capacity of 1000 kN was placed on one side of the brackets. The steel brackets *6* were equipped with steel pistons *7* articulated (jointed) with the dynamometer and the actuator on one side and steel sheets *12* on the other, to transmit load from hydraulic actuators to the tested block and to measure loading. Load transmitted to sheets *12* was applied to the tested block through Teflon slabs *11* eliminating any friction. Standard stresses σ_3 perpendicular to the face of masonry unit were induced in the same way as towards perpendicular direction to the bed surface. However, steel brackets *10* equipped with an actuator *8a* with the capacity of 300 kN on one side and a dynamometer *9a* with the capacity of 250 kN on another side, were fixed to the column *15* of the testing machine by means of steel clamps *14*. The load was transmitted with steel pistons *7* to the sheets *12*. Also friction at the face was maximally reduced by placing Teflon washers *11* on both sides of the masonry unit.

The tests were conducted on sixteen masonry units grouped into four series marked as TSB-I, TSB-IIa, TSB-IIb and TSB-III. TSB-I series included five masonry units, for which the vertical stress σ_{ver} was increasing until their failure at constant horizontal stresses $\sigma_{rad,I} = \sigma_{rad,II} = 0.007f_c; 0.009f_c; 0.08 f_c; 0.12f_c; 0.18f_c$.

To reduce the impact of shear stresses induced by non-uniform loading of blocks, at the initial phase vertical and horizontal stresses were gradually increased until achieving the assumed value of horizontal stress σ_{rad} . Then, the masonry units were loaded by increasing vertical stress σ_{ver} , until failure was observed while values of assumed horizontal stresses were monitored. TSB-IIa series included three masonry units exposed to increased horizontal stress $\sigma_{rad,I}$ until failure was observed. Other areas of those units were not loaded. TSB-IIb series included three masonry units destroyed by increasing horizontal stress $\sigma_{rad,II}$ acting on side face of bricks. Other areas of those units were not loaded.

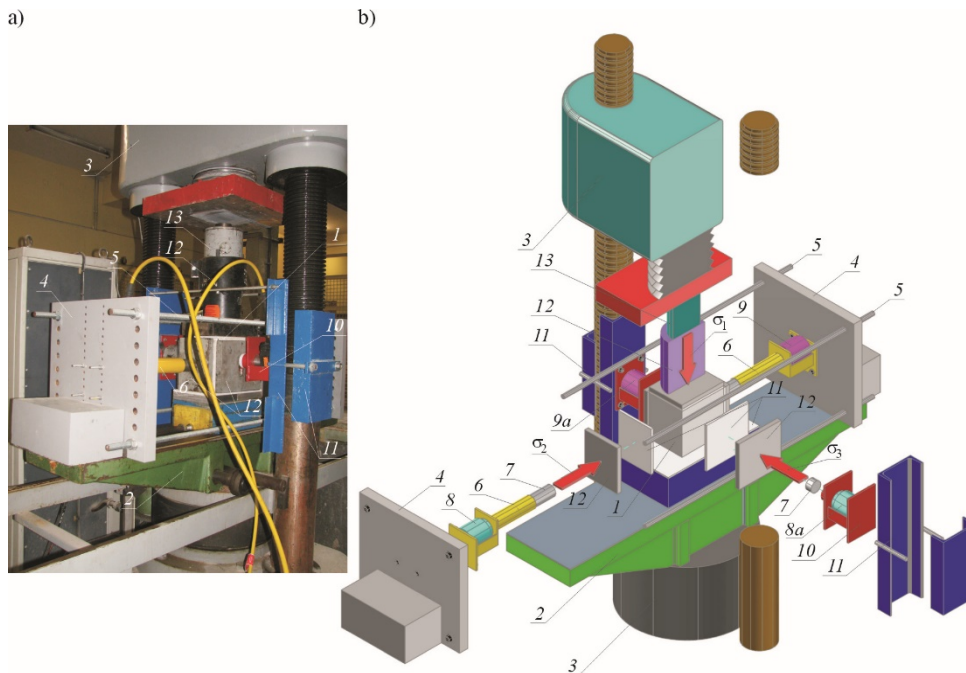


Fig. 3. Test stand for masonry units exposed to triaxial stress a) overall view, b) components of the test stand (described in the text)

TSB-III series included five masonry units, whose failure was achieved by increasing horizontal stress $\sigma_{rad,I}$ along a longer axis of the block (according to arrangement in the masonry) and vertical stress to meet the following condition $\sigma_{rad,I} = \sigma_{ver}$ during the tests. Stresses perpendicular to the side face of the unit were $\sigma_{rad,II} = 0$. For the purpose of reducing the impact of shear stresses induced by uniaxial load applied to the units from TSB-III series, horizontal and vertical stresses were applied uniformly until the unit failure was observed.

As it was impossible to observe the sample during the tests, the moment of their failure was determined on the basis of measured loads. Failure was regarded as a clear force drop (readable from the dynamometer). Fig. 4 presents results for measured horizontal and vertical stresses for all samples from TSB-I and TSB-III series. The summary of results is shown in Table 2.

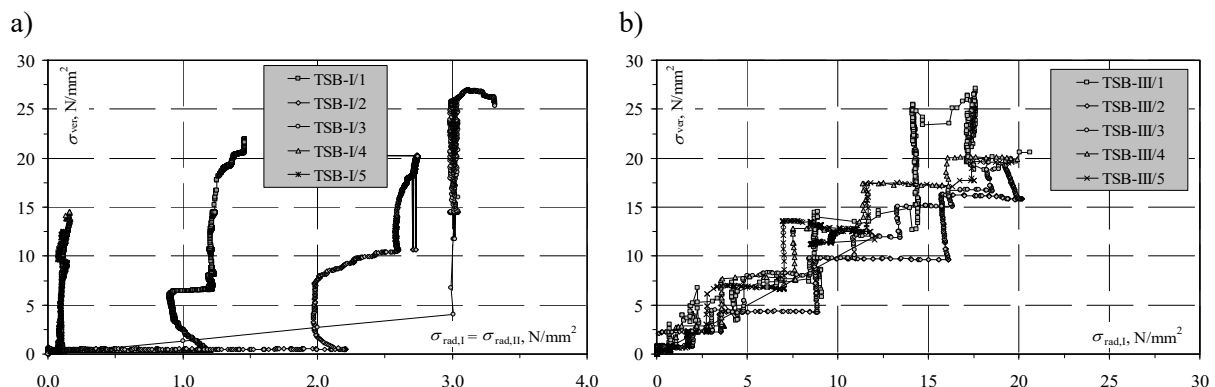


Fig. 4 Relationship $\sigma_{ver}-\sigma_{rad}$ of tested masonry units from TSB-I and TSB-III series: a) $\sigma_{rad,I} = \sigma_{rad,II} = \text{const.}$, b) $\sigma_{ver} = \sigma_{rad,I}$

At the lowest horizontal stresses, not exceeding 1% of compressive strength of blocks from TSB-I series, vertical stresses at failure contributed to 71%-82% of compressive strength. Vertical stresses

were greater than compressive strength of the unit by 20% on average when horizontal stresses contributed to 10% of the compressive strength. For the units from TSB-III series, whose failure was induced by increasing vertical and horizontal stresses perpendicular to the head surface of the units, the vertical stress at failure was greater than compressive strength by 11%. When uniaxial tests inducing stresses perpendicular to the head or side face of the unit were performed, stresses at failure contributed to 29% of the compressive strength (for TBS-IIa series), and to 43% (for TBS-IIb series). The failure of masonry units from TSB-I series induced by increasing stress vertical at the constant horizontal stresses was similar as that of units in the uniaxial compression. No clear failure was observed on the support area - Fig. 5a. Another failure mechanism was found in the units from TSB-III series to which increasing vertical and horizontal stresses were applied. At the failure moment – Fig. 5b, cracks were found on each external side of the unit. Internal walls between cavities were almost completely crushed.

Table 2. Results from triaxial tests on silicate masonry units

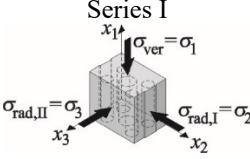
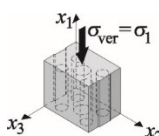
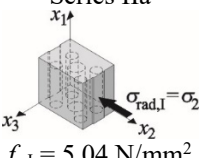
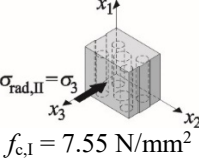
Meridian	Series	Specimen identification	Vertical stress			Horizontal stress		Haigh-Westergaard coordinates	
			$\sigma_{ver} = \sigma_1$ N/mm ²	$\sigma_{rad,I} = \sigma_2$ N/mm ²	$\sigma_{rad,II} = \sigma_3$ N/mm ²	ζ N/mm ²	ρ N/mm ²		
Compressive meridian	 <p>Series I</p>	TSB-I/1	21.95	1.46	1.46	14.36	16.73		
		TSB-I/2	20.26	2.11	2.11	14.13	14.82		
		TSB-I/3	26.95	3.12	3.12	19.16	19.46		
		TSB-I/4	14.54	0.16	0.16	8.58	11.74		
		TSB-I/5	12.51	0.12	0.12	7.36	10.12		
	 <p>Axial compression $f_{c,I} = 17.7$ N/mm²</p>	1	18.23	0	0	10.53	14.88		
		2	17.78	0	0	10.27	14.52		
		3	17.38	0	0	10.03	14.19		
		4	18.02	0	0	10.40	14.71		
		5	17.76	0	0	10.25	14.50		
		6	16.93	0	0	9.77	13.82		
	 <p>Series IIa $f_{c,I} = 5.04$ N/mm²</p>	TSB-IIa/1	0	5.03	0	2.90	4.10		
		TSB-IIa/2	0	4.37	0	2.52	3.57		
		TSB-IIa/3	0	5.73	0	3.31	4.68		
	 <p>Series IIb $f_{c,I} = 7.55$ N/mm²</p>	TSB-IIb/1	0	0	7.38	4.26	6.0		
		TSB-IIb/2	0	0	7.25	4.19	5.9		
		TSB-IIb/3	0	0	8.00	4.62	6.5		

Table 2 continued. Results from triaxial tests on silicate masonry units

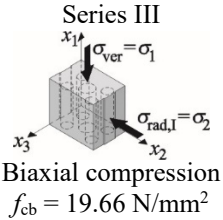
Meridian	Series	Specimen identification	Vertical stress			Horizontal stress			
			$\sigma_{ver} = \sigma_1$ N/mm ²	$\sigma_{rad,I} = \sigma_2$ N/mm ²	$\sigma_{rad,II} = \sigma_3$ N/mm ²	ζ N/mm ²	ρ N/mm ²		
Tensile meridian	 <p>Series III Biaxial compression $f_{cb} = 19.66 \text{ N/mm}^2$</p>	TSB-III/1	20.63	20.63	0	23.82	-16.84		
		TSB-III/2	19.27	19.27	0	22.25	-15.74		
		TSB-III/3	18.88	18.88	0	21.80	-15.41		
		TSB-III/4	19.90	19.90	0	22.98	-16.25		
		TSB-III/5	19.60	19.60	0	22.63	-16.00		
		1	$f_t \frac{f_b}{f_B} =$ $= 1,92 \frac{17,7}{24,5} = 1,39$			0	0	-0.80	-1.13
		2	0	$1,92 \frac{5,04}{17,7} =$ $= 0,55$			0	-0.316	-0.45
		3	0	0	$1,92 \frac{7,55}{17,7} =$ $= 0,82$			-0.47	-0.67



Fig. 5 Relationship of tested masonry units from TSB-I and TSB-III series: a) $\sigma_{rad,I} = \sigma_{rad,II} = \text{const.}$, b) $\sigma_{ver} = \sigma_{rad,I}$

4. Calibration of failure surface

Considering the discussed criterion, the shape of meridians forming the failure surface is not subjected to any modifications as it is determined by uniaxial compression and tension. However, some shape corrections of M-W-3 failure surface as well adjustments to results from testing other material than concrete are possible. Corrections involve eccentricity e of elliptical function, which determines the shape of failure surface at deviatory cross-section. The properly chosen eccentricity value of elliptical function should ensure that uniaxial tensile strength and biaxial compressive strength are as close as possible to tensile meridian, and the compressive strength is distributed at or as close as possible to the compressive meridian.

Iterative procedure, based on searching the optimum shape of compressive and tensile meridians, was used to determine the value e . Changes in the value e were used to calculate the biaxial compressive strength f_{cb} , which was compared with the strength observed in the tests. Every time a standard error in estimating the shape of meridians with reference to the obtained test results, was calculated on the basis of results from triaxial tests. The value e , at which the lowest percentage difference was obtained, was assumed in further numerical calculations.

At first, Haigh-Westergaard coordinates (ξ , ρ , Θ) were used to present the obtained stress values acc. to the following equations:

$$\xi = \frac{I_1}{\sqrt{3}}, \quad (4)$$

$$\rho = \sqrt{2J_2}, \quad (5)$$

$$\Theta = \frac{1}{3} \arccos \left[\frac{3\sqrt{3}J_3}{2J_2^{2/3}} \right], \quad (6)$$

where:

$I_1 = \sigma_1 + \sigma_2 + \sigma_3$ – first invariant of stress,

$J_2 = \frac{1}{6} [(\sigma_1 - \sigma_2)^2 + (\sigma_2 - \sigma_3)^2 + (\sigma_3 - \sigma_1)^2]$ – second invariant of stress,

$J_3 = (\sigma_1 - \sigma_m)(\sigma_2 - \sigma_m)(\sigma_3 - \sigma_m)$ – second invariant of stress,

$\sigma_m = \frac{1}{3} I_1$ – average hydrostatic pressure

$\sigma_1 = \sigma_{\text{ver}}$ – vertical stress (perpendicular to the supporting plane for silicate units),

$\sigma_2 = \sigma_{\text{rad,I}}$ – horizontal stress (perpendicular to the supporting plane for silicate units).

$\sigma_3 = \sigma_{\text{rad,II}}$ – horizontal stress (perpendicular to the bed plane for silicate units).

Load paths ($\sigma_{\text{ver}} > \sigma_{\text{rad}}$ – TSB-I, TSB-IIa and TSB-IIb series, and $\sigma_{\text{ver}} = \sigma_{\text{rad}}$ – series III) found in the planes inside the failure surface were used in triaxial tests on silicate units. For $\sigma_{\text{ver}} < \sigma_{\text{rad}}$, the values of points corresponding to sample failure were at the compressive meridian for which Lodge angle was $\Theta = 60^\circ$. If $\sigma_{\text{ver}} = \sigma_{\text{rad}}$, points identifying the strength were placed at the tensile meridian, for which Lodge angle was $\Theta = 0^\circ$. In case of autoclaved aerated concrete, two series of tests were performed. They included samples collected at various combinations of vertical and horizontal stresses. For TABK-I series, vertical stresses was increased at the constant horizontal stresses ($\sigma_{\text{ver}} > \sigma_{\text{rad}}$), and points distributed at the compressive meridian were identified at failure moment. For TABK-II series, the sample failure was caused by increasing horizontal stresses at the constant vertical stresses ($\sigma_{\text{ver}} < \sigma_{\text{rad}}$) and points at the tensile meridian were also identified.

Apart from the points determined from the triaxial tests, also results from uniaxial tests on compression and tension were necessary for calibrating the eccentricity of elliptical function. For that purpose, horizontal stress was assumed as $\sigma_{\text{rad}} = 0$. Tensile strength values for silicate units were determined from sampled cores in axial tension. Then, tensile strength ratios along the axis of masonry

units (also acting as orthotropic axes) were assumed to be identical with the compressive strength. Thus, strength values along the axis of masonry units were calculated by multiplying the determined axial tensile strength of block material by the ratio of compressive strength towards a given direction to compressive strength of whole masonry units observed in the tests. Due to isotropy of AAC material, uniaxial compressive and tensile strength did not require any corrections and they were directly assumed in the tests.

The summary of test results is presented in Table 2, and calculations of meridian shapes area shown in Table 3. Fig. 6 illustrates test results and trajectory of compressive and tensile meridians calculated from the following expression:

Compressive meridian

$$\rho_c(\xi, r_c) = \frac{\sqrt{6}}{36} \left(-2r_c k(\kappa) f_c m + 2\sqrt{r_c^2 (k(\kappa) f_c)^2 m^2 - 12\sqrt{3} m k(\kappa) f_c \xi + 36c(\kappa) (k(\kappa) f_c)^2} \right), \quad (7)$$

Tensile meridian

$$\rho_t(\xi, r_t) = \frac{\sqrt{6}}{36} \left(-2r_t k(\kappa) f_c m + 2\sqrt{r_t^2 (k(\kappa) f_c)^2 m^2 - 12\sqrt{3} m k(\kappa) f_c \xi + 36c(\kappa) (k(\kappa) f_c)^2} \right), \quad (8)$$

where:

r_c – parameter of elliptical function at compressive meridian calculated from the equation (3) at Lodge angle $\Theta=60^\circ$,

r_t – parameter of elliptical function at tensile meridian calculated from the equation (4) at Lodge angle $\Theta=0^\circ$,

$$m = 3 \frac{(k(\kappa) f_c)^2 - (\lambda_t f_t)^2}{k(\kappa) f_c \lambda_t f_t} \frac{e}{e+1} - \text{cohesion equivalent},$$

$k(\kappa)=1$ – strengthening parameter at plasticisation moment,

$c(\kappa)=1$ – weakening parameter at plasticisation moment,

$\lambda_t = 1$ – scaling parameter of boundary surface.

f_c, f_t – uniaxial compressive and tensile strength,

The comparison of triaxial test results for silicate units and AAC with calculations based on M-W-3 surface at different values e is shown in Table 3. In addition to biaxial compression $f_{bc,cal}$ identified from the compressive meridian, there are also triaxial uniform values for triaxial uniform tensile $f_{tt,cal}$ which is the intersection of meridians at the plane of hydrostatic tension. At $e = 0.52$ being the default eccentricity value for standard concrete, biaxial compressive strength of silicate units calculated from the equation for tensile meridian differed from empirical value by 36%, and the standard estimating error was 14.2%. By reducing eccentricity to the value $e = 0.51$, analogously determined biaxial compressive strength was lower than the empirical by only 10%, and the standard estimating error was 14.1%. A trial and test method indicated that the best strength adjustment to biaxial compression with the difference to mean value from the tests at the level of 2%, was obtained at eccentricity $e = 0.504$, and standard estimating error equal to 14.1%.

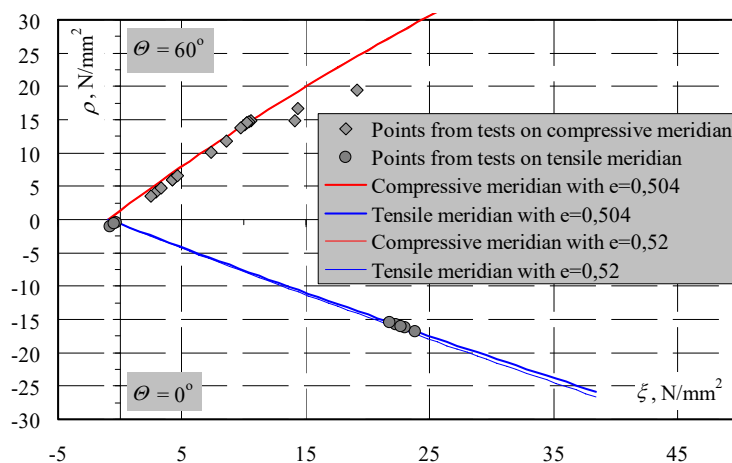


Fig. 6. Uniaxial and triaxial test results and compressive and tensile meridians of M-W-3 boundary surface

Table 3. Comparison of uniaxial and biaxial tests with calculations based on M-W-3 surface at different values of parameter e

Material	Test results			Parameter e	Calculated results		$\frac{f_{bc}}{f_{bc,cal}}$	standard estimating error was B , %
	$f_{b,mv}$, N/mm ²	$f_{bt,mv}$, N/mm ²	f_{bc} , N/mm ²		$f_{fit,cal}$, N/mm ²	$f_{bc,cal}$, N/mm ²		
silicate blocks	17.7	0.55	19.7	0.504	0.943	19.26	1.02	14.1
				0.51	0.936	21.86	0.90	14.1
				0.52	0.92	26.72	0.74	14.2

5. Conclusions

Uniaxial and triaxial tests were necessary for identifying each failure surface in the Haigh–Westergaard (H-W) space. For homogeneous materials such as concrete or rock, typical chamber pressures e.g. Hoek or Karman could be used. Standard methods were not effective for masonry units. Therefore, other techniques are required. Failure surface of silicate units was identified by means of the test stand for masonry units in triaxial stress, especially developed for the purpose of testing such materials. The obtained test results were expressed as H-W coordinates, and the value of parameter e was chosen iteratively to the failure surface M-W-3. The determined value was equal to $e=0.504$, which approximated the shape of surface M-W-3 at deviatoric cross-section to the equilateral triangle. However, that result was differed from the default value for concrete, which was $e = 0.52$. In contrast to concrete, the parameter e determined for masonry units could not be regarded as the constant value attributed to a specific type of materials. For brick, eccentricity of elliptical function was determined within the range of $e = 0.501 - 0.511$. Considerably greater spread of values could be expected in case of units with vertical cavities.

References

- [1] Jasiński R., Drobiec Ł., Piekarczyk A.: „Mechanical Properties of Masonry Walls Made of Calcium Silicate Materials Made in Poland. Part 1. Masonry Properties and Compressive Strength”. *Procedia Engineering* Volume 161, 2016, pp. 904÷910 (item bib 13). DOI: 10.1016/j.proeng.2016.08.755.
- [2] Jasiński R., Drobiec Ł., Piekarczyk A.: „Mechanical Properties of Masonry Walls Made of Calcium Silicate Materials Made in Poland. Part 2. Shear and Flexural Strength”. *Procedia Engineering* Volume 161, 2016, pp. 911÷917 (item bib 15). DOI: 10.1016/j.proeng.2016.08.756.

- [3] Drobiec Ł., Jasiński R.: „The failure surface of the masonry made of hollow silicate units”. *International Conference on Analytical Models and New Concepts in Concrete and Masonry Structures, Gliwice 2017*.
- [4] Menétrey P., Willam K.J.: „Triaxial failure criterion for concrete and its generalization”. *ACI Structural Journal*, Vol 92, No. 3/1995, pp. 311–318.
- [5] Hoek E., Brown E. T.: Empirical Criterion for Rock Masses. *Journal of the Geotechnical Engineering Division*, Vol. 106, No. GT9/1980, pp. 1013 – 1035.
- [6] Weihe S.: „Implicit Integration Schemes for Multi-Surface Yield Criteria Subjected to Hardening/Softening Behavior”. MS thesis. University of Colorado-Bulder, 1989.
- [7] Drobiec Ł.: „FEM Micro-Model for Masonry Reinforced in Bed Joints”. *Proceedings of the British Masonry Society*, No. 10, October/November 2006, Published by the Society Stoke-on-Trent.
- [8] Jasiński R.: Numerical model of the horizontally sheared wall. *7th International Conference analytical Models and New Concepts in Concrete and Masonry Structures AMCM 2011*, pp. 233–234.